A seven-sex species recognizes self and non-self mating-type via a novel protein complex

Guanxiong Yan[1], Yang Ma[1], Yanfang Wang[2], Jing Zhang[1], Haoming Cheng[1, 3], Fanjie Tan[2], Su Wang[1, 3], Delin Zhang[2], Jie Xiong[1], Ping Yin[2]*, Wei Miao[1, 3, 4, 5]*

[1] Institute of Hydrobiology, Chinese Academy of Sciences, Wuhan 430072, China

[2] National Key Laboratory of Crop Genetic Improvement, Hubei Hongshan Laboratory, Huazhong Agricultural University, Wuhan 430070, China

[3] University of Chinese Academy of Sciences, Beijing 100049, China

[4] State Key Laboratory of Freshwater Ecology and Biotechnology of China, Wuhan 430072, China

[5] CAS Center for Excellence in Animal Evolution and Genetics, Kunming 650223, China

Corresponding author: Wei Miao, miaowei@ihb.ac.cn.

Ping Yin, yinping@mail.hzau.edu.cn.

Abstract

Although most species have two sexes, multisexual species (i.e., those with multiple mating types) are also widespread. However, it is unclear how mating-type recognition is achieved at the molecular level in multisexual species. The unicellular ciliate *Tetrahymena thermophila* has seven mating types, which are determined by the MTA and MTB proteins. In this study, we found that both proteins are essential for cells to send or receive complete mating-type information, and transmission of the mating-type signal requires both proteins to be expressed in the same cell. We found that MTA and MTB form a mating-type recognition complex that localizes to the plasma membrane, but not to the cilia. Stimulation experiments showed that the mating-type-specific regions of MTA and MTB mediate both self- and non-self-recognition, indicating that *T. thermophila* uses a dual approach to achieve mating-type recognition. Our results suggest that MTA and MTB form an elaborate multifunctional protein complex that can identify cells of both self and non-self mating types in order to inhibit or activate mating, respectively.

Impact statement

A giant multifunctional protein complex mediates mating-type recognition through a non-ligand-receptor mechanism in a multisexual species.

35 ## Introduction

36 Sexual reproduction is almost universal among eukaryotic organisms. Mating type (or sex) is
37 a key regulatory feature of gamete fusion. Most species have only two mating types (e.g., male
38 and female, + and -, or a and α) and species usually use either self- or non-self-recognition
39 mechanism to achieve mating-type recognition (Goodenough & Heitman, 2014). However,
40 species in some lineages, such as some ciliates and basidiomycetes (Heitman, 2015; Phadke &
41 Zufall, 2010), possess multiple mating types, and multiple-alleles self-incompatibility system
42 were observed in some plants, such as Brassicaceae (Iwano & Takayama, 2012; Takayama &
43 Isogai, 2005; Vekemans & Castric, 2021). This raises the interesting question of how mating types
44 are recognized at the molecular level in multiple mating-type systems.

45 The model unicellular ciliate, *Tetrahymena thermophila*, has seven mating types (I–VII).
46 Under starvation conditions, any cell of one mating type can mate with a cell of any of the other
47 six mating types, but not with one of the same mating type (Figure 1A, Figure 1–figure
48 supplement 1, Video 1–3) (Cervantes et al., 2013; Nanney, 1953; Orias et al., 2017; Yan et al.,
49 2021). Mating-type recognition in *Tetrahymena* depends on direct cell–cell contact, which
50 suggests that mating-type proteins localize to the cell surface. However, there is no direct
51 evidence to indicate whether they are ciliary proteins or not. When one cell comes into contact
52 with a cell of a different mating type, a mating-type-dependent recognition event enables both
53 cells to enter a pre-conjugation stage (called costimulation) (Bruns & Palestine, 1975; Finley &
54 Bruns, 1980). Even when cells of different mating types are mixed in unequal ratios (for example,
55 9 : 1), all cells become fully stimulated (Bruns & Palestine, 1975). Processes that take place

56 during costimulation include Tip transformation (Wolfe & Grimes, 1979) and concanavalin A
57 (Con-A) receptor appearance (Figure 1B) (Wolfe & Feng, 1988; Wolfe et al., 1986). In preparation
58 for pairing, costimulated cells of the same and different mating type(s) adhere to form very loose
59 pairs. Heterotypic cell pairs form a stable conjugation junction, whereas homotypic pairs
60 separate very quickly (Video 2 and 3) (Kitamura et al., 1986).

61 The mating-type system of *T. thermophila* was described by Nanney and collaborators in the
62 early 1950s (reviewed in (Orias, 1981; Orias et al., 2017)). We previously showed that mating
63 type is determined by a pair of mating-type genes that are organized in head-to-head
64 orientation: *MTA* and *MTB* (Figure 1C) (Cervantes et al., 2013). Each gene has a terminal exon
65 that encodes five transmembrane (TM) helices and a cysteine-rich growth factor receptor (GFR)
66 domain. The region between the two terminal exons of the gene pair encodes the N-terminal
67 mating-type-specific extracellular regions. Based on the mating-type-specific regions, the mating-
68 type genes are called *MTA1-MTB1* for Mating type I, *MTA2-MTB2* for Mating type II and so on.
69 We previously showed that Δ*MTB* cells do not form pairs or produce progeny and that Δ*MTA*
70 cells retain mating-type specificity but pair extremely poorly and rarely produced progeny
71 (Cervantes et al., 2013); we concluded that the two genes are non-redundant and both are
72 essential for mating. However, challenges such as multiple mating types; the high molecular
73 weight, membrane localization and extremely low expression levels of mating-type proteins; and
74 difficulty in genetically manipulating the mating-type gene locus have so far prevented
75 elucidation of the mode of action of the MTA and MTB proteins and of whether they mediate
76 self- or non-self mating-type recognition.

77 In this study, we provide direct evidence that the MTA and MTB form an elaborate
78 multifunctional protein complex that can identify cells of both self and non-self mating types to
79 inhibit or activate mating, respectively.

80 ## Results

81 **Mating-type recognition cannot be explained by a simple receptor–ligand model**

82 Receptor–ligand interactions are a critical mechanism for intercellular communication that
83 may regulate mating-type recognition in *T. thermophila*, irrespective of whether self- or non-self-
84 recognition mechanisms are employed. Therefore, we first assessed whether mating-type
85 recognition conforms to a straightforward receptor–ligand model (in which one mating-type
86 protein acts as the receptor and the other as the ligand) and whether self or non-self is
87 recognized (Figure 2–figure supplement 1A, 1 and 2). For this, we determined whether deletion
88 of each mating-type gene affected the transmission and detection of mating signals to and from
89 wild-type (WT) cells (Figure 2A shows the experimental procedure) by assessing the ability of
90 cells to undergo costimulation (the prerequisite for mating). Our experiment allows us to test if
91 cells missing one of the two mating-type proteins can still costimulate WT cells (Figure 2–figure
92 supplement 1A, 3 and 6).

93 In *T. thermophila*, cells normally enter into the fully costimulation stage within ~30 min after
94 mixing starved WT cells of two different mating types, and start pair formation during the next
95 ~30 min (Figure 2B, black line). Cells that have already been costimulated immediately start
96 forming pairs with other costimulated cells of a different mating type (Figure 2B, red line).

97 To our surprise, the rate of pair formation in WT cells pre-incubated with either Δ*MTA* cells
98 (Figure 2B, green line) or Δ*MTB* cells (Figure 2B, blue line) did not increase (i.e., costimulation did
99 not occur). These results were not changed by extending the pre-incubation time (Figure 2–
100 figure supplement 1B). Therefore, both MTA and MTB proteins are essential for the mating-type
101 signal; there is no simple receptor–ligand relationship.

102 In addition, WT cells were not costimulated even when they were simultaneously incubated
103 with both Δ*MTA* and Δ*MTB* cells (Figure 2B, teal line), although, according to the receptor–ligand
104 model, they should have received "MTA stimulation" from Δ*MTB* cells and "MTB stimulation"
105 from Δ*MTA* cells. This result indicates that the absence of a mating-type protein in one cell
106 cannot be complemented by its presence in another cell in the same culture; the MTA and MTB
107 proteins must be in the same cell to transmit the mating-type signal. This finding suggests that
108 mating-type recognition cannot be explained by a simple receptor–ligand model. It is possible
109 that the MTA and MTB proteins form a complex which either serves as a recognizer (functioning
110 as both ligand and receptor) or a co-receptor (which influences ligand–receptor activity). But,
111 since MTA and MTB are the only genes with mating-type-specificity, it is unlikely that the
112 complex is acting as a co-receptor.

113 **Mating-type proteins differentially regulate two steps of costimulation**

114 During costimulation, cells undergo a sequence of developmental events that remodel the
115 anterior cell membrane and its associated cytoskeleton (Cole, 2013). Two hallmarks of this
116 process are Tip transformation (in which the anterior tip of the cell becomes curved) and Con-A

117 receptor appearance (receptors bound by the plant lectin concanavalin A, which binds to
118 mannose containing glycoproteins). When WT cells of one mating type were mixed with WT cells
119 of another mating type, the cell tips became transformed (Figure 2C, 5 and 9) and Con-A
120 receptors appeared in almost all cells (Figure 2D, 4). When WT cells were pre-incubated with
121 Δ*MTA*, Δ*MTB*, or both cell types, Tip transformation was not observed in any cell (Figure 2C, 6–
122 8). Similarly, when cells of each mutant were pre-incubated with WT cells, Tip transformation
123 was not detected (Figure 2C, 10 and 11). The outcome was slightly different for Con-A receptor
124 appearance. Con-A receptors were not observed in WT cells pre-incubated with Δ*MTB* cells
125 (Figure 2D, 6) or in cells of either mutant pre-incubated with WT cells (Figure 2D, 7 and 8). In
126 contrast, when WT cells were exposed to Δ*MTA* or "Δ*MTA* cells plus Δ*MTB* cells", the Con-A
127 receptor was detected (Figure 2D, 5 and 9); this is consistent with Δ*MTA* cells retaining a very
128 weak ability to pair (Cervantes et al., 2013). These results indicate that neither Δ*MTA* and Δ*MTB*
129 cells can fully stimulate WT cells or be stimulated by WT cells. They also demonstrate that
130 costimulation can be separated into two stages: (i) the appearance of Con-A receptors, which
131 requires the expression of MTB only in partner cells, and (ii) morphological transformation of the
132 cell tip, which requires both MTA and MTB.

133 **Mating-type proteins form a complex with several coexpressed proteins**

134 The inability of "Δ*MTA* cells plus Δ*MTB* cells" to costimulate WT cells of a different mating
135 type indicates that MTA and MTB proteins can only function when expressed on the same cell
136 (Figure 2B, teal; Figure 2C, 8). We previously found that CDK19 and CYC9 proteins are also

137 essential for mating. Δ*CDK19* and Δ*CYC9* cells cannot mate with other cells, but they still express
138 MTA and MTB proteins (Ma et al., 2020). In WT cells, the pairing rate was increased following
139 pre-incubation with Δ*CDK19* or Δ*CYC9* cells of a different mating type (Ma et al., 2020). These
140 results further support the idea that MTA and MTB must be expressed on the same cell to be
141 fully functional, leading us to hypothesize that MTA and MTB proteins form a mating-type
142 recognition complex (MTRC).

143 To test whether MTA and MTB proteins physically interact, an HA-tag coding sequence was
144 ligated to the 3' end of the *MTA* gene (Figure 3A); cellular proteins were co-precipitated with HA-
145 tagged MTA and analyzed by immunoprecipitation-coupled mass spectrometry (IP-MS). As
146 expected, the MTB protein co-purified with MTA (Figure 3B, C), as did another set of proteins,
147 which we named MRC1–MRC6 (Figure 3B, C and Figure 3–Source data 1 and 2). Next, we
148 produced strains expressing either HA-tagged MTB or MRC1 (Figure 3A), and found that each
149 protein pulled down a subset of the proteins that co-purified with MTA (Figure 3B, C).
150 Unfortunately, these pull-down experiments were not as successful as the MTA IPs, perhaps
151 because of the higher molecular weight of MTB and MRC1. Taken together, our results suggest
152 that MTA, MTB, and MRC1–MRC6 form the MTRC. Alternatively, MTA and MTB may interact with
153 subsets of MRC proteins to form smaller complexes or alternative MTRCs. Different protein
154 interactors were identified in extracts from cells at different mating stages. This may reflect
155 conformational changes in the MTRC but the huge molecular weight of the complex and
156 extremely low expression levels of its proteins make this possibility difficult to investigate.

157 Mating-type-related factors in other species are often relatively small (Iwano & Takayama,
158 2012; Kahmann & Bölker, 1996), but those of *T. thermophila* are large proteins (predicted size,
159 92–212 kDa). Figure 3D shows the predicted domains of the MRC1–MRC6 proteins. Like MTA and
160 MTB, MRC1 has five predicted TM helices and a GFR domain. MRC2 has eight TM helices and a
161 pectin lyase-fold domain, suggesting a possible role in carbohydrate chain modification. MRC3
162 has two TM helices in the central region and an adjacent ~35 amino acid (aa) poly-E region.
163 MRC4 and MRC5 (previously named TPA9 (Wang et al., 1997; Wang & Takeyasu, 1997)) are both
164 P-type ATPases that are likely to function as calcium-translocators. MRC6 has four TM helices and
165 a P-loop containing nucleoside triphosphate hydrolases. Most of the MRC genes are highly
166 coexpressed with *MTA* and *MTB* (Figure 3E). Examination of the whole genome sequences of
167 strains with mating types II–VII (Wang et al., 2020), confirmed that only the sequences of *MTA*
168 and *MTB* genes are mating-type-specific.

169 In addition to the MRC proteins, CDK19, CYC9, CIP1, and AKM3 were identified in IP-MS
170 experiments, but with relatively few supporting peptides (Figure 3C). Our previous work showed
171 that CDK19, CYC9, and CIP1 are components of a cyclin-dependent kinase complex. These genes
172 are coexpressed with *MTA* and *MTB* (Figure 3E) and are important for mating, and the encoded
173 proteins localize to the cell tip and pairing junction (Ma et al., 2020). AKM3 is predicted to be a K^+
174 channel of unknown biological function. It is coexpressed with *MTA* and *MTB* (Figure 3E), and we
175 found that the *AKM3* deletion strain cannot pair. Therefore, these four proteins are also likely to
176 interact with the mating-type proteins (perhaps indirectly and/or via weak interactions) and
177 might be involved in downstream signaling following mating-type recognition.

178 **Mating-type proteins localize to the cell surface but not to the cilia**

179 We used the MTA7-HA strain to determine the localization of mating-type proteins. Cell
180 fractionation (Figure 4–figure supplement 1) revealed that MTA7-HA is a membrane protein
181 (Figure 4A). Biotinylation and isolation of cell surface proteins confirmed that MTA7-HA is
182 exposed on the cell surface (Figure 4B). To investigate whether MTA7-HA localizes to the cilia
183 membrane, we isolated and collected cilia (Figure 4C) and then analyzed cilia protein extracts by
184 IP-coupled western blotting (WB) and MS. MS analysis identified typical ciliary proteins, such as
185 inner and outer arm dynein proteins (Figure 4–Source data 1). However, both IP-WB (Figure 4D)
186 and MS (Figure 4–Source data 1) consistently failed to identify MTA7-HA protein in the cilia
187 fraction. These results conclusively indicate that MTA7-HA localizes to the cell surface, but not to
188 cilia. Unfortunately, we failed to detect MTA7-HA by immunofluorescence staining of cells at any
189 mating stage (starvation, costimulation, or conjugation), probably due to the epitope masking
190 and extremely low expression level.

191 To further examine localization of the mating-type proteins, eGFP-tagged MTB2 was
192 overexpressed from an exogenous locus (Figure 4E). This strain (which has a mating type VI
193 background) mated normally with WT cells of all mating types except for VI and II. This result
194 indicates the overexpressed MTB2-eGFP protein is fully functional for mating. Interestingly, cells
195 of this strain can also mate with one another (self-mating); a similar phenotype was previously
196 reported for strains expressing multiple mating-type proteins (Lin & Yao, 2020). The
197 overexpressed MTB2-eGFP protein was detected on the cell surface in a linear pattern radiating
198 from the cell tip to the cell body along the ciliary rows (Figure 4F, costimulated cell; Figure 4G,

199 mating pair), although signals are also apparent between ciliary rows. Co-staining with a tubulin
200 dye showed that the MTB2-eGFP protein is adjacent to, rather than co-localizing with, the base
201 of cilia (Figure 4F, G, enlarged). Confocal images from the interior of the cell and through the cilia
202 showed that MTB2-eGFP localizes to the cell surface (and also to intracellular structures,
203 probably the endoplasmic reticulum (ER) and Golgi), but not to the cilia (Figure 4–figure
204 supplement 2), confirming our results with the MTA7-HA protein (Figure 4A-D). MS analysis
205 showed that overexpressed MTB2-eGFP protein was not present in isolated cilia of the *MTB2-*
206 *eGFP* strain (Figure 4–Source data 2). Therefore, mating-type proteins localize to the cell surface,
207 as might be expected since mating-type recognition depends on cell–cell contact.

208 **Mating-type proteins influence non-self-recognition**

209 The mating-type-specific region of the *MTA* and *MTB* gene pair is the only known genetic
210 locus with mating-type specificity; therefore, we next tested whether this region influences self-
211 and/or non-self mating-type recognition. For this, we expressed the extracellular region of MTA
212 (MTAxc) or MTB (MTBxc) in an insect cell secreted expression system, purified the recombinant
213 proteins (Figure 5–figure supplement 1), and then tested their effect on mating behavior.

214 First, we tested whether MTAxc and MTBxc can influence mating in cells with a different
215 mating-type specificity (i.e., non-self-recognition). When WT cells were incubated with MTAxc
216 (and/or MTBxc) of a different mating type, markers of costimulation were not observed (Figure
217 5–figure supplement 2). Surprisingly, treated cells had a significantly increased pairing rate.
218 Compared with controls (Figure 5A–C, black), WT cells (VI and VII) pre-treated with MTAxc or
219 MTBxc of different mating types (VII and VI, respectively) had an increased pairing rate

220 (Figure 5A–C, green or blue), with a stronger effect after pre-treatment with both MTAxc and
221 MTBxc (Figure 5A–C, teal). Dose–effect assays showed that pairing rates increased with
222 increasing MTA6xc and MTB6xc concentrations between 3 pg/ml and 30 pg/ml, with the effect
223 becoming saturated or weaker at higher concentrations (Figure 6A–F). MTAxc and MTBxc also
224 stimulated mating for all other WT mating types (Figure 6G, H), indicating that this is a general
225 effect. Based on these results, we conclude that the mating-type-specific regions of MTA and
226 MTB proteins are involved in non-self mating-type recognition.

227 **Mating-type proteins also influence self-recognition**

228 We used similar methods to examine whether pre-treatment with a cognate mating-type-
229 specific region (i.e., self-recognition) affects mating. Treatment of WT cells (VI and VII) with
230 MTAxc and/or MTBxc of the same mating type decreased the pairing rate (Figure 5D, E, green or
231 blue). No obvious difference was found between treatments with either MTAxc or MTBxc.
232 Meanwhile, a significant synergistic effect was observed (Figure 5D, E, teal). For all treatments
233 (single or combined), the pairing rate was similar by 4 h (reaching >80%; Figure 5D, F), indicating
234 that the initial inhibitory effect on pairing was eventually overcome. Negative regulation by
235 MTAxc and MTBxc was also observed for other mating-type combinations (Figure 6I, J). These
236 results support the idea that the mating-type-specific regions of MTA and MTB proteins mediate
237 both non-self (between cells of different mating types) and self (between cells of same mating
238 type) recognition.

239 ## Discussion

240 Although the basic biological features of the *T. thermophila* mating-type system were
241 discovered over half a century ago, the mechanism for mating-type recognition remains unclear.
242 Here, we identified a novel MTRC that contains MTA, MTB, and several other proteins and
243 provide evidence that MTA and MTB mediate both self and non-self mating-type recognition.

244 In most species, mating signals are associated with relatively small proteins or molecules
245 (Iwano & Takayama, 2012; Kahmann & Bölker, 1996). However, in *T. thermophila*, the MTRC is
246 likely to be over a million Daltons in size. This large size is consistent with its multiple functions:
247 An elaborate MTRC is needed to inhibit mating between cells of the same mating type while also
248 activating mating between cells of different mating types. This is likely to be a highly complex
249 process, given that there are seven mating types in all. Further structural studies of this protein
250 complex may reveal the specific self- and non-self-recognition mechanisms.

251 An open question is why *T. thermophila* should use such a dual approach to achieving
252 mating-type recognition. Recent research on basidiomycetes and flowering plants (other species
253 with multiple mating types) has shown that their mating-type recognition (or self-
254 incompatibility) mechanisms involve either self- or non-self-recognition (Fraser & Heitman, 2003;
255 Iwano & Takayama, 2012; Vekemans & Castric, 2021). Our previous evolutionary study showed
256 that the length of the mating-type-specific region differs significantly among different
257 *Tetrahymena* species (Yan et al., 2021). Based on the massive difference in length, it is
258 reasonable to speculate that different species might use different mechanisms for mating-type
259 recognition. Therefore, dramatic evolution of the mating-type recognition mechanism seems to

260 have occurred relatively soon after the emergence of the *Tetrahymena* genus. Further detailed
261 functional and evolutionary studies may reveal how and why this recognition mechanism
262 evolved and how its evolution contributed to speciation.

263 We still do not know what intracellular signals are transduced when the MTRCs on two cells
264 interact. Mating-type self-recognition might generate an inhibitory signal or might simply
265 inactivate the MTRC. In many species, such as *Papaver rhoeas* and *Ciona intestinalis*, interaction
266 between mating-type proteins of the same mating type induces changes in cytoplasmic Ca^{2+}
267 concentration that cause self-incompatibility (Giamarchi et al., 2006; Harada et al., 2008; Wu et
268 al., 2011). A similar system may exist in *T. thermophila*, since the MRC4 and MRC5 proteins are
269 predicted to be Ca^{2+}-translocators. Interaction between MTRCs on cells of different mating types
270 (non-self-recognition) should result in their activation to allow the cells to initiate pairing. We
271 propose that the activation signal involves the CDK19 complex (a cyclin-dependent kinase
272 complex) (Ma et al., 2020) and AKM3 (a K^+ channel; Figure 3C) because they probably interact
273 with the MTRC. We expect future studies to lead to the discovery of more detailed mechanisms
274 for mating-type recognition and initiation of conjugation involving these proteins.

275 *Paramecium tetraurelia*, a closely related Oligohymenophorean ciliate, has only two mating
276 types, which are determined by the expression or non-expression of a *Tetrahymena*-MTA/B-like
277 protein called mtA (Singh et al., 2014; Yan et al., 2021). An intriguing question is whether mtA
278 also engages in the formation of a MTRC with other proteins by serving as a recognizer rather
279 than mediating a straightforward receptor–ligand interaction. Future investigations of
280 *Paramecium tetraurelia* may shed light on the origins and evolutionary aspects of this distinctive

281 mating system. Moreover, due to the extremely long evolutionary distance, recognition
282 mechanisms discovered in model species fall short of explaining many of the intricate biological
283 events in protists. Insight into the detailed function of MTRC could contribute to our
284 understanding of cell–cell recognition processes in other species, such as *Toxoplasma* and
285 *Plasmodium*.

286 ## Materials and Methods

287 **Biological methods**

288 Strains used in this study are summarized in Appendix 1–table 1. All cell growth, starvation, and
289 pairing experiments were conducted at 30°C. Cells were grown in Super Proteose Peptone (SPP)
290 medium (1% Proteose Peptone, 0.1% yeast extract, 0.2% glucose, 0.003% Sequestrene) or Neff
291 medium (0.25% Proteose Peptone, 0.25% yeast extract, 0.5% glucose, 0.003% Sequestrene). Cells
292 were starved in 10 mM Tris-Cl (pH 7.4) for ~16 h before all pairing experiments. For normal
293 pairing assays, equal numbers of starved cells of different mating types (at ~2×10^6 cells/ml) were
294 mixed. To obtain costimulated (pre-incubated) cells, two starved strains were mixed at a 9 : 1
295 ratio for ~30 min (unless otherwise stated). Before mixing costimulated cells, any potentially
296 pairing cells were separated by shaking. Figure 2A shows the setup of costimulation experiments.
297 For all mating experiments (whether or not they involved mutant cells), the starting WT cell
298 density was ~2×10^6 cells/ml. The following formula was used to calculate pairing ratios and
299 correct for the presence of mutant cells:

300 $$\%cells\ paired = \frac{2 \times \#\ pairs}{(2 \times \#\ pairs + \#\ unpaired\ cells) \times \%\ WT\ cells} \times 100$$

301 **Somatic gene deletion, truncation, and protein tagging**

302 To construct deletion strains, a ~1 kb fragment upstream of the gene's open reading frame (ORF)
303 (#1), a ~0.5 kb fragment downstream of the gene's ORF (#2), and a ~1 kb fragment downstream
304 of #2 (#3) were amplified. Fragments #2 and #3 were joined to the *NEO4* cassette (Cd^{2+}-inducible
305 *MTT1* promoter linked to the neomycin resistance gene) by fusion PCR and then cloned into the
306 pBlueScript SK (+) vector together with fragment #1. In this way, #1-#2-*NEO4*-#3 constructs were
307 obtained for the next transformation. HA-tagged strains were constructed in a similar way,
308 except that fragment #1 was upstream of the stop codon or upstream of the terminal intron. To
309 obtain the MTB2-eGFP construct, MTB2-coding sequences replaced the MTT1-coding sequence
310 (Figure 4E) and the construct was made using the large DNA fragment assembly method (Jiang et
311 al., 2022). Constructs were introduced into starved WT cells by biolistic transformation to obtain
312 deletion strains (Mochizuki, 2008). Positive clones were selected in SPP medium containing
313 decreasing Cd^{2+} concentrations (from 1 μg/ml to 0.05 μg/ml) and increasing paromomycin
314 concentrations (from 120 μg/ml to 40 mg/ml) until all WT somatic chromosomes had been
315 replaced by mutant ones, as determined by PCR using checking primers. All primers used are
316 listed in Appendix 1–table 2.

317 **Immunoprecipitation and mass spectrometry**

318 The IP method was adapted from a published method (Tian et al., 2017). To pull down HA-tagged
319 proteins from *T. thermophila*, cells were harvested from 500 ml cultures (density
320 ~3×10^6 cells/ml). Cells were then treated for 20 min with paraformaldehyde (PFA) (at a final
321 concentration of 0.3%) to stabilize protein–protein interactions, washed with PB buffer (2.7 mM
322 KCl, 8 mM Na_2HPO_4, 1.5 mM K_2HPO_4), and blocked with 125 mM glycine. Cells were then

323 resuspended in lysis buffer (1% Triton X-100, 30 mM Tris-HCl, 20 mM KCl, 2 mM $MgCl_2$, 1 mM
324 phenylmethylsulfonyl fluoride, 150 mM NaCl, cOmplete proteinase inhibitor [Roche Diagnostics,
325 Indianapolis, IN, USA]), lysed by ultrasonic treatment and incubated with EZview anti-HA agarose
326 beads (Sigma-Aldrich, St Louis, MO, USA) for 2.5 h at 4°C. The beads were washed with wash
327 buffer (1% Triton X-100, 600 mM NaCl, 30 mM Tris-HCl, 20 mM KCl, 2 mM $MgCl_2$, cOmplete
328 proteinase inhibitor) to remove nonspecific-binding proteins and then HA-tagged proteins were
329 eluted with HA peptides (Sigma-Aldrich). WT samples (not HA tagged) were run in parallel for
330 each sample. In total, data for 13 WT controls were combined to identify non-specific binding
331 proteins.

332 For MS, the EASY-nLC chromatography system (Thermo Scientific, Rockford, IL, USA) was
333 coupled on-line to an Orbitrap Elite instrument (Thermo Scientific) via a Nanospray Flex Ion
334 Source (Thermo Scientific). Xtract software (Thermo Scientific) and Proteome Discoverer 2.1
335 software were used for MS data analysis based on a database that combines the 2014 version of
336 whole genome protein annotation (http://ciliate.org/index.php/home/downloads, which
337 contains the whole length sequence of MTA6 and MTB6) and mating-type-specific regions of all
338 other mating-type proteins. IP data were analyzed using CRAPome (Mellacheruvu et al., 2013).

339 **Membrane protein extraction**

340 Figure 4–figure supplement 1A shows the workflow used for membrane protein extraction. Cells
341 were collected, resuspended in 20 ml lysis buffer (150 mM NaCl, 25 mM HEPES, 10% glycerol,
342 2 mM PMSF, 2.6 µg/ml aprotinin, 1.4 µg/ml pepstatin, 10 µg/ml leupeptin, pH 7.4), and lysed by
343 high-pressure homogenization. The lysate was clarified first at low speed (14,000 rpm, 4°C,

344 15 min), and then at high speed (150,000 g, 4°C, 1 h). The pellet was resuspended in 5 ml lysis
345 buffer containing 1% DDM (Anatrace, Maumee, OH, USA) and rotated for 2 h at 4°C to extract
346 the membrane proteins. Undissolved material was removed by centrifugation (14,000 rpm, 4°C,
347 30 min). The membrane protein extract was incubated with EZview anti-HA agarose beads for
348 2.5 h at 4°C and then washed with 5 ml lysis buffer.

349 **Biotinylation and isolation of cell surface proteins**

350 Pierce Cell Surface Protein Biotinylation and Isolation Kit (Thermo Scientific) was used to
351 biotinylate and isolate cell surface proteins. For this, 75 ml cells (density ~3×10^6 cells/ml) were
352 harvested and washed once with BupH phosphate-buffered saline (PBS; 137 mM NaCl, 2.7 mM
353 KCl, 4.3 mM Na_2HPO_4, 1.4 mM KH_2PO_4). Cells were then resuspended in 75 ml PBS containing
354 0.72 mg/ml Sulfo-NHS-SS-biotin and incubated at room temperature for 10 min. After two
355 washes with 50 ml ice-cold BupH Tris buffer, cells were resuspended in 3 ml lysis buffer (PBS
356 containing 1% Triton X-100, 1 mM phenylmethylsulfonyl fluoride and cOmplete proteinase
357 inhibitor [Roche Diagnostics]), lysed by ultrasonic treatment and incubated with 1.2 ml
358 NeutrAvidin Agarose for 0.5 h at room temperature. The resin was washed four times with 0.5 ml
359 wash buffer and then cell surface proteins were eluted with 1.2 ml elution buffer (with 10 mM
360 DTT). Before WB, cell surface protein samples were concentrated into 0.1 ml volumes using a
361 30 kDa centrifugal concentrator (Merck Millipore).

362 **Ciliary protein collection**

363 To remove cilia, 500 ml cells (density ~3×10^6 cells/ml) were harvested at room temperature and
364 resuspended in 25 ml 10 mM Tris-Cl (pH 7.4), to which 50 ml medium A (10 mM $EDTA_2Na$,

365 50 mM sodium acetate, pH 6.0) was added. After 30 s, 25 ml cold distilled water was added;
366 1 min later, 0.25 ml 0.4 M $CaCl_2$ was added and incubated for 15 s. The cilia were detached from
367 the calcium-shocked cells by vortexing three times for 5 s at 15 s intervals. To collect the cilia, cell
368 bodies were removed by two rounds of centrifugation at 1500 rpm for 5 min at 4°C, and then
369 cilia were collected by centrifugation at 15000 rpm for 15 min at 4°C.

370 **Cytological methods**

371 For tubulin staining, cells were collected and fixed in PHEM buffer (30 mM PIPES, 14 mM HEPES,
372 5 mM EGTA and 2 mM $MgSO_4$) containing 1% PFA and incubated for 30 min at 4°C. After three
373 washes with PBS (10 min each), Tubulin-Atto 594 was added and incubated for 1 h at 25°C.
374 Finally, cells were washed three times with PBS (10 min each). Fluorescein-labeled Con-A labeling
375 was performed as previously reported (Ma et al., 2020). In brief, cells were fixed and stained
376 with fluorescein-labeled Con-A (Vector Laboratories, Burlingame, CA, USA) at 37.5 μg/ml for
377 5 min and then washed three times with PB. For analysis of Tip transformation, cells were
378 observed and photographed as soon as possible after fixation with 1% PFA. To distinguish
379 between cell strains in a pairing mixture, starved cells of one strain were labeled with 500 nM
380 MitoTracker (Invitrogen, Eugene, OR, USA), followed by two washes with 10 mM Tris-Cl (pH 7.4)
381 before mixing.

382 **Expression and purification of the extracellular region of mating-type proteins**

383 Coding sequences of the extracellular region of mating-type proteins (MTA6xc, MTB6xc, MTA7xc,
384 and MTB7xc) were codon-optimized and synthesized for expression in an insect-cell system
385 (*Trichoplusia ni* Hi5 cells). Codon-optimized sequences were cloned into pFastBac vectors

386 containing an N-terminal hemolin signal peptide sequence and a C-terminal 10×His tag sequence.
387 The obtained constructs were transformed into competent DH10Bac cells and individual bacmids
388 were transfected into *Spodoptera frugiperda* Sf9 cells. Recombinant Baculoviruses were
389 collected after 4 days and used to infect *Trichoplusia ni* Hi5 cells for protein expression. Proteins
390 were harvested 60 h after infection and purified with Ni-NTA Superflow resin (Qiagen), anion-
391 exchange chromatography (Source 15Q, GE Healthcare), and size-exclusion chromatography
392 (Superdex-200 Increase 10/300, GE Healthcare).

393 **Bioinformatics analysis**

394 All microarray data were derived from *Tetra*FGD (Xiong et al., 2011) (http://tfgd.ihb.ac.cn/). DNA
395 sequencing data for mating type II–VII cells are derived from a previous report (Wang et al.,
396 2020). Compute pI/Mw (https://web.expasy.org/compute_pi/) was used to predict protein
397 molecular weight. InterProScan (http://www.ebi.ac.uk/interpro/) was used for function and
398 domain annotation (Jones et al., 2014).

399 **Statistical analysis**

400 For mating experiments, more than 100 unpaired cells or cell pairs were counted, with three to
401 five independent replicates. GraphPad software (version 8.0.2) was used for statistical analysis
402 based on ANOVA (matched, Fisher's LSD test).

403 **Acknowledgments**

404 We thank Eduardo Orias (University of California Santa Barbara), Eileen P. Hamilton (University of
405 California Santa Barbara), and Kazufumi Mochizuki (University of Montpellier) for their help and
406 suggestions about experiment design and manuscript writing, and Yunfei Wei (Huazhong

University of Science and Technology) for tubulin staining using Tubulin-Atto 594. We also thank members of the Protist 10,000 Genomes Project (P10K) consortium for helpful suggestions. We would like to thank Min Wang at the Analysis and Testing Center of Institute of Hydrobiology, Chinese Academy of Sciences for her help with mass spectrometry. The bioinformatics analysis was supported by the Wuhan Branch, Supercomputing Center, Chinese Academy of Sciences, China. Culture and maintenance of *Tetrahymena* cells were supported by the National Aquatic Biological Resource Center (NABRC).

Funding information

This work was funded by Bureau of Frontier Sciences and Education, Chinese Academy of Sciences (No. ZDBS-LY-SM026), National Natural Science Foundation of China (No. 32130011, 32200344) and China Postdoctoral Science Foundation (No. 2021M703433).

Author Contributions

G.Y. performed the experiments and analyzed the data. Y.M and H.C helped to construct mutants and perform cellular experiments. Y.W. and F.T. performed protein expression and purification experiments. J.Z helped to maintenance of *Tetrahymena* strains. G.Y. wrote the manuscript. All of the authors helped to conceptualize the work, and edit the text and the figures. W.M. and P.Y. supervised the work.

Conflict of Interest

Authors declare that they have no competing interests.

References

427 Adair, W. S., Barker, R., Turner, R. S., & Wolfe, J. (1978). Demonstration of a cell-free factor involved in
428 cell interactions during mating in *Tetrahymena*. *Nature*, *274*(5666), 54-55.
429 Bruns, P. J., & Palestine, R. F. (1975). Costimulation in *Tetrahymena pyriformis*: A developmental
430 interaction between specially prepared cells. *Developmental Biology*, *42*(1), 75-83.
431 https://doi.org/https://doi.org/10.1016/0012-1606(75)90315-2
432 Cervantes, M. D., Hamilton, E. P., Xiong, J., Lawson, M. J., Yuan, D., Hadjithomas, M., Miao, W., &
433 Orias, E. (2013). Selecting one of several mating types through gene segment joining and
434 deletion in *Tetrahymena thermophila*. *PLOS Biology*, *11*(3), e1001518.
435 https://doi.org/10.1371/journal.pbio.1001518
436 Cole, E. S. (2013). *The Tetrahymena Conjugation Junction. In: Madame Curie Bioscience Database*
437 *[Internet].* Landes Bioscience.
438 Finley, M. J., & Bruns, P. J. (1980). Costimulation in *Tetrahymena* II. A nonspecific response to
439 heterotypic cell-cell interactions. *Developmental Biology*, *79*(1), 81-94.
440 https://doi.org/https://doi.org/10.1016/0012-1606(80)90074-3
441 Fraser, J. A., & Heitman, J. (2003). Fungal mating-type loci. *Current Biology*, *13*(20), R792-795.
442 https://doi.org/10.1016/j.cub.2003.09.046
443 Fujishima, M., Tsuda, M., Mikami, Y., & Shinoda, K. (1993). Costimulation-induced rounding in
444 *Tetrahymena thermophila*: early cell shape transformation induced by sexual cell-to-cell
445 collisions between complementary mating types. *Developmental Biology*, *155*(1), 198-205.
446 https://doi.org/10.1006/dbio.1993.1018
447 Giamarchi, A., Padilla, F., Coste, B., Raoux, M., Crest, M., Honore, E., & Delmas, P. (2006). The versatile
448 nature of the calcium-permeable cation channel TRPP2. *EMBO Reports*, *7*(8), 787-793.
449 https://doi.org/10.1038/sj.embor.7400745
450 Goodenough, U., & Heitman, J. (2014). Origins of eukaryotic sexual reproduction. *Cold Spring Harbor*
451 *Perspectives in Biology*, *6*(3). https://doi.org/10.1101/cshperspect.a016154
452 Harada, Y., Takagaki, Y., Sunagawa, M., Saito, T., Yamada, L., Taniguchi, H., Shoguchi, E., & Sawada, H.
453 (2008). Mechanism of self-sterility in a hermaphroditic chordate. *Science*, *320*(5875), 548-
454 550.
455 Heitman, J. (2015). Evolution of sexual reproduction: a view from the Fungal Kingdom supports an
456 evolutionary epoch with sex before sexes. *Fungal Biology Reviews*, *29*(3-4), 108-117.
457 https://doi.org/10.1016/j.fbr.2015.08.002
458 Iwano, M., & Takayama, S. (2012). Self/non-self discrimination in angiosperm self-incompatibility.
459 *Current Opinion in Plant Biology*, *15*(1), 78-83. https://doi.org/10.1016/j.pbi.2011.09.003
460 Jiang, S., Tang, Y., Xiang, L., Zhu, X., Cai, Z., Li, L., Chen, Y., Chen, P., Feng, Y., Lin, X., Li, G., Sharif, J., &
461 Dai, J. (2022). Efficient de novo assembly and modification of large DNA fragments. *Sci China*
462 *Life Sci*, *65*(7), 1445-1455. https://doi.org/10.1007/s11427-021-2029-0
463 Jones, P., Binns, D., Chang, H. Y., Fraser, M., Li, W., McAnulla, C., McWilliam, H., Maslen, J., Mitchell,
464 A., Nuka, G., Pesseat, S., Quinn, A. F., Sangrador-Vegas, A., Scheremetjew, M., Yong, S. Y.,
465 Lopez, R., & Hunter, S. (2014). InterProScan 5: genome-scale protein function classification.
466 *Bioinformatics*, *30*(9), 1236-1240. https://doi.org/10.1093/bioinformatics/btu031

467 Kahmann, R., & Bölker, M. (1996). Self/Nonself Recognition in Fungi: Old Mysteries and Simple
468 Solutions. *Cell*, *85*(2), 145-148. https://doi.org/https://doi.org/10.1016/S0092-
469 8674(00)81091-0
470 Kitamura, A., Sugai, T., & Kitamura, Y. (1986). Homotypic pair formation during conjugation in
471 *Tetrahymena thermophila*. *Journal of Cell Science*, *82*, 223-234.
472 Lin, I. T., & Yao, M. C. (2020). Selfing mutants link Ku proteins to mating type determination in
473 *Tetrahymena*. *PLOS Biology*, *18*(8), e3000756. https://doi.org/10.1371/journal.pbio.3000756
474 Ma, Y., Yan, G., Han, X., Zhang, J., Xiong, J., & Miao, W. (2020). Sexual cell cycle initiation is regulated
475 by CDK19 and CYC9 in *Tetrahymena thermophila*. *Journal of Cell Science*, *133*(6).
476 https://doi.org/10.1242/jcs.235721
477 Mellacheruvu, D., Wright, Z., Couzens, A. L., Lambert, J. P., St-Denis, N. A., Li, T., Miteva, Y. V., Hauri,
478 S., Sardiu, M. E., Low, T. Y., Halim, V. A., Bagshaw, R. D., Hubner, N. C., Al-Hakim, A.,
479 Bouchard, A., Faubert, D., Fermin, D., Dunham, W. H., Goudreault, M., . . . Nesvizhskii, A. I.
480 (2013). The CRAPome: a contaminant repository for affinity purification-mass spectrometry
481 data. *Nature methods*, *10*(8), 730-736. https://doi.org/10.1038/nmeth.2557
482 Mochizuki, K. (2008). High efficiency transformation of *Tetrahymena* using a codon-optimized
483 neomycin resistance gene. *Gene*, *425*(1-2), 79-83.
484 https://doi.org/10.1016/j.gene.2008.08.007
485 Nanney, D. L. (1953). Nucleo-Cytoplasmic Interaction during Conjugation in *Tetrahymena*. *Biological*
486 *Bulletin*, *105*(1), 133-148. https://doi.org/10.2307/1538562
487 Orias, E. (1981). Probable somatic DNA rearrangements in mating type determination in *Tetrahymena*
488 *thermophila*: A review and a model. *Developmental Genetics*, *2*(2), 185-202.
489 https://doi.org/doi:10.1002/dvg.1020020205
490 Orias, E., Cervantes, M. D., & Hamilton, E. P. (2011). *Tetrahymena thermophila*, a unicellular
491 eukaryote with separate germline and somatic genomes. *Research in Microbiology*, *162*(6),
492 578-586. https://doi.org/10.1016/j.resmic.2011.05.001
493 Orias, E., Singh, D. P., & Meyer, E. (2017). Genetics and Epigenetics of Mating Type Determination in
494 *Paramecium* and *Tetrahymena*. *Annual Review of Microbiology*, *71*(1).
495 Phadke, S. S., & Zufall, R. A. (2010). Rapid diversification of mating systems in ciliates. *Biological*
496 *Journal of the Linnean Society*, *98*(1), 187-197.
497 Singh, D. P., Saudemont, B., Guglielmi, G., Arnaiz, O., Gout, J. F., Prajer, M., Potekhin, A., Przybos, E.,
498 Aubusson-Fleury, A., Bhullar, S., Bouhouche, K., Lhuillier-Akakpo, M., Tanty, V., Blugeon, C.,
499 Alberti, A., Labadie, K., Aury, J. M., Sperling, L., Duharcourt, S., & Meyer, E. (2014). Genome-
500 defence small RNAs exapted for epigenetic mating-type inheritance. *Nature*, *509*(7501), 447-
501 452. https://doi.org/10.1038/nature13318
502 Takayama, S., & Isogai, A. (2005). Self-incompatibility in plants. *Annual Review of Plant Biology*, *56*(1),
503 467-489. https://doi.org/10.1146/annurev.arplant.56.032604.144249
504 Tian, M., Yang, W., Zhang, J., Dang, H., Lu, X., Fu, C., & Miao, W. (2017). Nonsense-mediated mRNA
505 decay in *Tetrahymena* is EJC independent and requires a protozoa-specific nuclease. *Nucleic*
506 *Acids Research*, *45*(11), 6848-6863. https://doi.org/10.1093/nar/gkx256

507 Vekemans, X., & Castric, V. (2021). When the genetic architecture matters: evolutionary and
508 ecological implications of self versus nonself recognition in plant self‐incompatibility. *New*
509 *Phytologist*, *231*(4), 1304-1307. https://doi.org/10.1111/nph.17471
510 Wang, G., Chen, K., Zhang, J., Deng, S., Xiong, J., He, X., Fu, Y., & Miao, W. (2020). Drivers of Mating
511 Type Composition in *Tetrahymena thermophila*. *Genome Biology and Evolution*, *12*(12),
512 2328-2343. https://doi.org/10.1093/gbe/evaa197
513 Wang, S., Gao, D., Penny, J., Krishna, S., & Takeyasu, K. (1997). P-Type ATPases in *Tetrahymena*.
514 *Annals of the New York Academy of Sciences*, *834*(1), 158-160.
515 https://doi.org/10.1111/j.1749-6632.1997.tb52247.x
516 Wang, S., & Takeyasu, K. (1997). Primary structure and evolution of the ATP-binding domains of the P-
517 type ATPases in *Tetrahymena thermophila*. *American Journal of Physiology*, *272*(2 Pt 1),
518 C715-728. https://doi.org/10.1152/ajpcell.1997.272.2.C715
519 Wolfe, J., & Feng, S. (1988). Concanavalin A receptor 'tipping' in *Tetrahymena* and its relationship to
520 cell adhesion during conjugation. *Development*, *102*(4), 699.
521 http://dev.biologists.org/content/102/4/699.abstract
522 Wolfe, J., & Grimes, G. W. (1979). Tip Transformation in *Tetrahymena*: A Morphogenetic Response to
523 Interactions Between Mating Types. *The Journal of Protozoology*, *26*(1), 82-89.
524 https://doi.org/10.1111/j.1550-7408.1979.tb02737.x
525 Wolfe, J., Pagliaro, L., & Fortune, H. (1986). Coordination of concanavalin-A-receptor distribution and
526 surface differentiation in *Tetrahymena*. *Differentiation*, *31*(1), 1-9.
527 https://doi.org/https://doi.org/10.1111/j.1432-0436.1986.tb00375.x
528 Wu, J., Wang, S., Gu, Y., Zhang, S., Publicover, S. J., & Franklin-Tong, V. E. (2011). Self-incompatibility
529 in *Papaver rhoeas* activates nonspecific cation conductance permeable to Ca2+ and K+. *Plant*
530 *Physiology*, *155*(2), 963-973. https://doi.org/10.1104/pp.110.161927
531 Xiong, J., Lu, X., Lu, Y., Zeng, H., Yuan, D., Feng, L., Chang, Y., Bowen, J., Gorovsky, M., Fu, C., & Miao,
532 W. (2011). *Tetrahymena* Gene Expression Database (TGED): a resource of microarray data
533 and co-expression analyses for *Tetrahymena*. *Sci China Life Sci*, *54*(1), 65-67.
534 https://doi.org/10.1007/s11427-010-4114-1
535 Yan, G., Yang, W., Han, X., Chen, K., Xiong, J., Hamilton, E. P., Orias, E., & Miao, W. (2021). Evolution of
536 the mating type gene pair and multiple sexes in *Tetrahymena*. *iScience*, *24*(1), 101950.
537 https://doi.org/10.1016/j.isci.2020.101950
538

539 ## Figure legends

540 **Figure 1. Mating-type recognition in *T. thermophila*.** (**A**) Example of self and non-self mating-
541 type recognition. When one cell of mating type I encounters another, costimulation and mating
542 do not occur. When a cell of mating type I encounters a cell of another mating type (II–VII), the
543 cells enter the costimulation stage and go on to form a pair. (**B**) Two typical phenotypes of the

544 costimulation stage are Tip transformation and Con-A receptor appearance. Yellow dashed circle,
545 transformed cell tip (center, single cell) or pairing junction (right, cell pair). Note that Tip
546 transformation may become less obvious after Con-A staining. (**C**) *MTA* and *MTB* gene structure
547 and MTA and MTB protein domain information (Cervantes et al., 2013). MTA and MTB form a
548 head-to-head gene pair. For each gene, the terminal exon is shared by all mating types and the
549 remainder is mating-type-specific (the sequence differs for each mating type). The mating-type-
550 specific region of each protein is predicted to be extracellular.

551 **Figure 2. Mating-type proteins are essential for mating-type recognition.** (**A**) Experimental
552 procedure for the costimulation experiments. Starved WT cells of mating types V (WT-V) and VII
553 (WT-VII) were separately pre-incubated with the indicated mating type VI mutant (9 : 1 ratio) for
554 30 min and then the pre-incubated cells were mixed at a 1 : 1 ratio. Note that before mixing the
555 costimulated cells, any potentially pairing cells were separated by shaking. (**B**) Effect of pre-
556 incubation with Δ*MTA* and Δ*MTB* on the rate of pair formation. Each experiment was repeated
557 three times, with > 100 pairs counted at each time point. Matched two-way ANOVA was used for
558 the statistical analysis. N.S., not significant; *, $P < 0.05$; **, $P < 0.01$; ***, $P < 0.001$; ****,
559 $P < 0.0001$. Unpaired mutants were excluded when calculating the pairing rate (see Materials
560 and Methods). (**C**) Tip transformation, a hallmark of costimulation. Costimulated cells from two
561 different WT strains are shown because their tips have slightly different shapes. Each strain was
562 pre-incubated with the strain shown in subscript. Yellow dashed circle, transformed cell tip. (**D**)
563 Appearance of Con-A receptors, another hallmark of costimulation. In all, ~90% cells show Con-A
564 receptor fluorescence (panels 4, 5 and 9). The low percentage of cells (7%) with fluorescence in

565 panel 7 were probably WT cells, which comprised 10% of the pre-incubation culture. Each strain
566 was pre-incubated with the strain shown in subscript. Yellow dashed circle, Con-A receptor
567 fluorescence.

568 **Figure 3. Proteins that interact with MTA and MTB.** (**A**) Construction of HA-tagged strains. All of
569 the tagged strains mated like WT cells. (**B**) Statistical analysis of IP-MS data. A total of 13
570 experiments were carried out. WT samples (untagged) were run in parallel for each sample. All
571 13 WT controls were combined as the background control. Red dot, high-confidence interaction;
572 dark gray dot, low-confidence interaction. Gene identifiers are summarized in Figure 3–Source
573 data 2. Note that the wash buffer contained 1% Triton X-100 and 600 mM NaCl. (**C**) Interaction
574 network based on IP-MS data. Orange oval, bait; blue oval, high-confidence prey; light gray dot,
575 low-confidence prey; black line, high-confidence interaction; dark gray dashed line, low-
576 confidence interaction; light gray dotted line, interaction supported by a few peptides (these
577 proteins were shown because their coding genes are coexpressed with *MTA* and *MTB* and
578 deleting them affects mating behavior). (**D**) Diagram of functional domain annotation of MTRC
579 components. GFR, growth factor receptor domain; PLF, pectin lyase fold; Poly-E, poly-glutamic
580 acid region; NTH, P-loop-containing nucleotide triphosphate hydrolase. (**E**) Expression profiles of
581 genes whose protein products were identified by IP-MS as potentially components of the MTRC.
582 Expression data is derived from *Tetra*FGD (Xiong et al., 2011).

583 **Figure 4. Mating-type proteins are cell surface proteins but do not localize to cilia.** (**A**)
584 Fractionation of *MTA7-HA* cells (please see Figure 4–figure supplement 1A for the experimental
585 process). Red arrowhead, MTA7-HA; F, flow through; P, pellet; R, resin; S, supernatant; W, wash.

586 The MTA signal is undetectable until S3 (enriched membrane proteins), and only appears after
587 affinity chromatography (R). (**B**) WB analysis of cell surface proteins. Red arrowhead, MTA7-HA;
588 M, marker; C, negative control (unbiotinylated). (**C**) Cilia isolation and purification. (**D**) WB
589 analysis of IP products of membrane and ciliary proteins. Mem, membrane; R, resin; S,
590 supernatant. The same amount of *MTA7-HA* cells was used for the membrane and ciliary protein
591 IPs. The full blot is shown in Figure 4–figure supplement 1B. (**E**) Construction scheme for eGFP-
592 tagged MTB2 strains. (**F**) Costimulated MTB2-eGFP cell. (**G**) Paired MTB2-eGFP cell. To induce
593 MTB2-eGFP overexpression, cells were treated with 10 ng/ml Cd^{2+} for 5 h. Green, eGFP signal;
594 red, tubulin signal; yellow dashed line, cell outline. The focal plane of these images is the cell
595 surface.

596 **Figure 5. Stimulation experiments using MTAxc and/or MTBxc.** (**A**) WT cells were treated with
597 MTAxc and/or MTBxc proteins (30 pg/ml, 1 h) of different mating-type specificities. WT-VI cells
598 were treated with MTA/B7xc protein, and WT-VII cells were treated with MTA/B6xc protein.
599 Treated cells were washed twice before mixing to remove residual proteins from the starvation
600 medium. Note that the starvation medium used for washing had been previously used for cell
601 starvation because *T. thermophila* cells secrete mating-essential factors during starvation (Adair
602 et al., 1978). Each experiment was repeated five times. (**B, C**) The percentages of cells paired at
603 60 min (**B**) and 75 min (**C**) were used for the statistical analysis (method described in Figure 2B).
604 (**D**) WT cells (mating types VI and VII) were treated with MTAxc and/or MTBxc proteins of the
605 same mating-type specificity (as described in (**A**)). (**E, F**) The percentages of cells paired at 75 min
606 (**E**) and 240 min (**F**) were used for the statistical analysis (method described in Figure 2B).

607 **Figure 6. Results of treatment with either MTAxc or MTBxc proteins.** (**A**–**F**) Dose–response
608 effect of treatment with MTA6xc or MTB6xc protein. (**A**–**C**) MTA6xc results. (**D**–**F**) MTB6xc
609 results. Cells of mating types I and VII were used for these experiments. Experimental and
610 statistical methods were as described for Figure 5, except for protein concentrations. (**G**–**J**)
611 MTA6xc or MTB6xc proteins affect the mating of various combinations of other WT mating types.
612 (**G**) MTA6xc results. Both mating partners were treated. (**H**) MTB6xc results. Both mating
613 partners were treated. (**I**) MTA6xc results. Cells of only one mating type were treated. Note that
614 mating type VI cells were used in these experiments. (**J**) MTB6xc results. Note that mating type VI
615 cells were used in these experiments. Experimental and statistical methods were as described for
616 Figure 5. Red superscript "T" in (**I**) and (**J**) indicate the strain treated with MTA6xc or MTB6xc.
617 The mating types used in each experiment is shown in the top-left corner.

618 ## Supplementary Information

619 **Figure 1 – figure supplement 1. *T. thermophila* lifecycle.** *T. thermophila* has seven mating types.
620 Cells divide asexually when nutrition is adequate. After starvation, cells of any two different
621 mating types recognize each other and enter a pre-conjugation stage called costimulation. In this
622 stage, cells first become round (Fujishima et al., 1993); subsequently, their cell tips are
623 transformed into a curved shape (Wolfe & Grimes, 1979) and the Con-A receptor becomes
624 detectable (Wolfe & Feng, 1988; Wolfe et al., 1986). Costimulated cells then form pairs via a
625 rotating behavior (Video S1, S2). During the sexual life cycle (conjugation), cells undergo a series
626 of sexual events such as meiosis and reciprocal fertilization (for details refer to (Orias et al.,
627 2011)). Exconjugants (separated pairs) finally form parent-like progeny when nutrition becomes

628 available, but remain sexually immature. After ~60 fissions, cells mature and their mating type is
629 determined and becomes fixed (for details of mating-type determination, refer to (Cervantes et
630 al., 2013; Lin & Yao, 2020; Orias et al., 2017)).

631 **Figure 2 – figure supplement 1. Mating-type gene deletion strains do not costimulate WT cells.**
632 (**A**) Pre-incubation results predicted by a simple receptor–ligand model of mating-type
633 recognition, in which one mating-type protein is designed ligand (L) and the other receptor (R).
634 The type of cell used to costimulate is shown on the left. The expected result of costimulation if
635 *T. thermophila* were to use non-self mating-type recognition (1, 3, 5) or self mating-type
636 recognition (2, 4, 6). If this simple model were true, deleting the receptor would have a different
637 effect on costimulation to deleting the ligand. However, the experimental results showed that
638 neither Δ*MTA* nor Δ*MTB* can fully transmit/receive mating signal to/from WT cells. Therefore,
639 mating-type recognition in *T. thermophila* does not occur via the simple receptor–ligand binding
640 mechanism. Costim, costimulation. (**B**) Pre-incubation with Δ*MTA* or Δ*MTB* does not influence
641 the pairing rate. The experimental method was as described in Figure 2A except that the pre-
642 incubation time was 16 h.

643 **Figure 4 – figure supplement 1. Cell fractionation MTA7-HA cells.** (**A**) Experimental process for
644 cell fractionation. (**B**) Affinity purification results of the soluble pool (S2, shown in panel A) and
645 ciliary protein. C+, positive control (i.e., IP product of MTA7-HA cell membrane); R, resin; S,
646 supernatant. No MTA7-HA signal was detected in the soluble pool or in ciliary protein samples,
647 even after affinity purification.

648 **Figure 4 – figure supplement 2. Confocal images of ciliary sections and cell interior sections of**
649 **MTB2-eGFP cells.** (**A**) No MTB2-eGFP signal was associated with cilia. (**B**) In the cell interior
650 section, MTB2-eGFP protein was detected on the plasma membrane and in intracellular
651 structures, probably the ER and Golgi.

652 **Figure 5 – figure supplement 1. Expression and purification of extracellular regions of mating-**
653 **type proteins.** (**A**) Schematic diagram showing truncated and full-sized proteins. (**B**–**E**) Size-
654 exclusion chromatography for MTA6xc (**B**), MTB6xc (**C**), MTA7xc (**D**), and MTB7xc (**E**). Left,
655 elution profile; right, Coomassie blue staining. In, input; M, marker.

656 **Figure 5 – figure supplement 2. Treatment with MTA6xc and/or MTB6xc proteins fails to**
657 **induce costimulation.** (**A**) Tip transformation. Yellow dashed circle, transformed cell tip. (**B**) Con-
658 A receptor appearance. Yellow dashed circle, Con-A signal. Cells of mating type VII were used for
659 these experiments.

660 **Video 1. Mating behavior of *T. thermophila*.**

661 **Video 2. Mating behavior of *T. thermophila*.** To distinguish cells of different mating types,
662 smaller mating type VI cells and larger mating type VII cells were used in this experiment.

663 **Video 3. Cells of different mating types form a pair, whereas cells of the same mating type**
664 **become separated after a short contact.** To distinguish cells of different mating types, smaller
665 mating type VI cells and larger mating type VII cells were used in this experiment.

666 **Figure 3–Source data 1. IP-MS results.**

667 **Figure 3–Source data 2. Gene identifiers.**

668 **Figure 4–Source data 1. MS analysis of MTA7-HA cilia protein.**

669 **Figure 4–Source data 2. MS analysis of MTB2-eGFP cilia protein.**

670 **Appendix 1—table 1. Strains used in this study.**

671 **Appendix 1—table 2. Primers used in this study.**

Figure 1

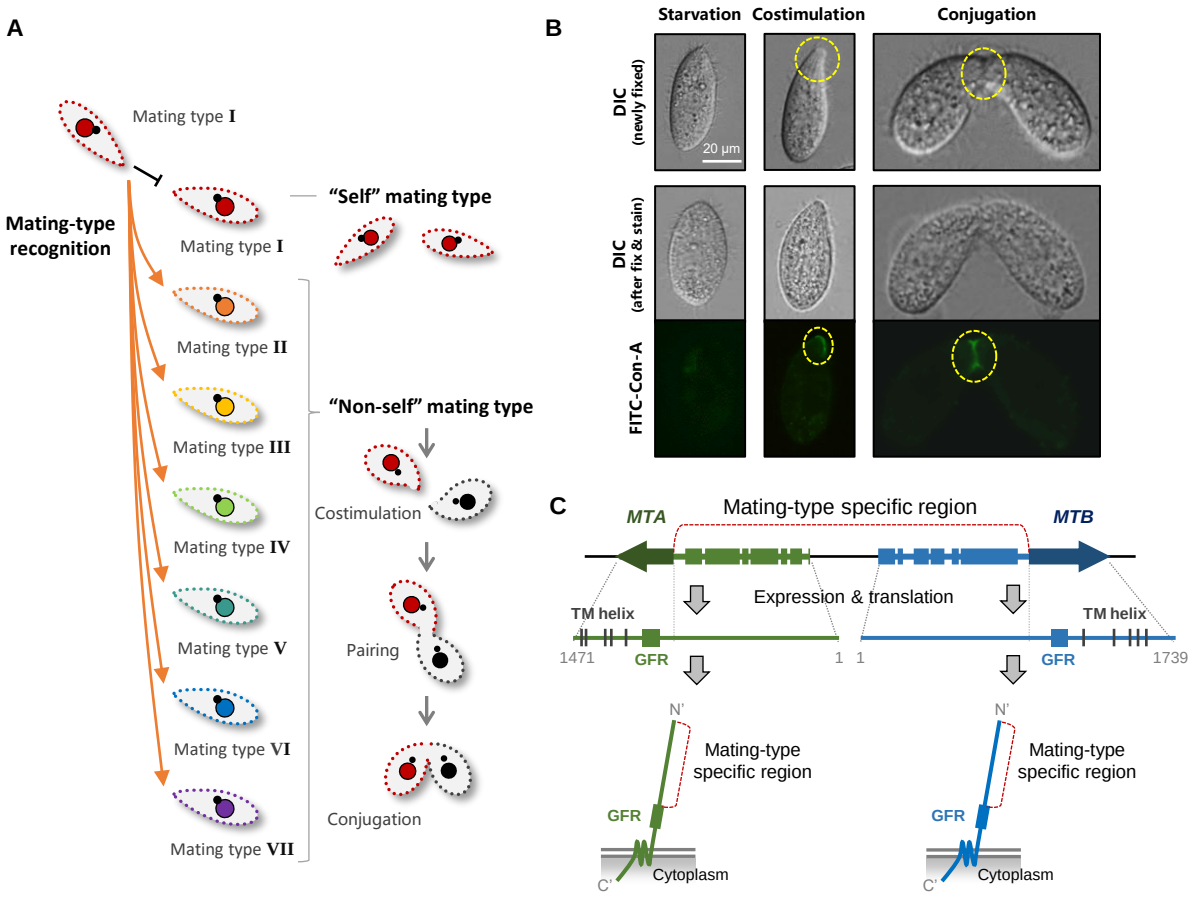
A
Mating type I
Mating-type recognition
Mating type I
"Self" mating type
Mating type II
Mating type III
"Non-self" mating type
Costimulation
Mating type IV
Mating type V
Pairing
Mating type VI
Conjugation
Mating type VII
B
Starvation
Costimulation
Conjugation
DIC (newly fixed)
20 µm
DIC (after fix & stain)
FITC-Con-A
C
MTA
Mating-type specific region
MTB
Expression & translation
TM helix
TM helix
1471
GFR
1
1
GFR
1739
N'
Mating-type specific region
GFR
Cytoplasm
C'
N'
Mating-type specific region
GFR
Cytoplasm
C'

Figure 2

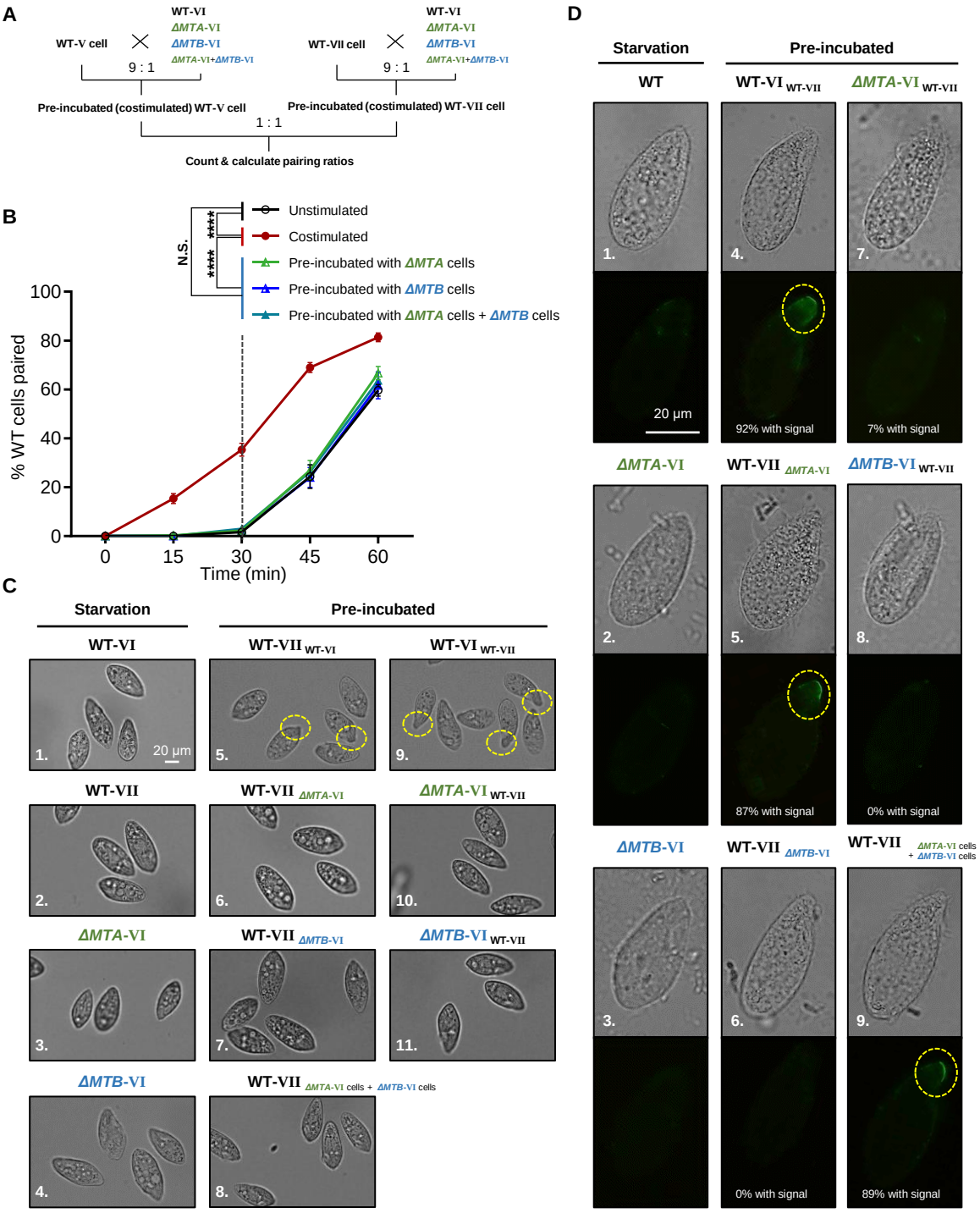
A
WT-V cell
WT-VI
ΔMTA-VI
ΔMTB-VI
ΔMTA-VI+ΔMTB-VI
9 : 1
Pre-incubated (costimulated) WT-V cell
WT-VII cell
WT-VI
ΔMTA-VI
ΔMTB-VI
ΔMTA-VI+ΔMTB-VI
9 : 1
Pre-incubated (costimulated) WT-VII cell
1 : 1
Count & calculate pairing ratios
B
Unstimulated
Costimulated
Pre-incubated with ΔMTA cells
Pre-incubated with ΔMTB cells
Pre-incubated with ΔMTA cells + ΔMTB cells
N.S.
****
****
% WT cells paired
100
80
60
40
20
0
0
15
30
45
60
Time (min)
C
Starvation
Pre-incubated
WT-VI
WT-VII WT-VI
WT-VI WT-VII
1.
20 µm
5.
9.
WT-VII
WT-VII ΔMTA-VI
ΔMTA-VI WT-VII
2.
6.
10.
ΔMTA-VI
WT-VII ΔMTB-VI
ΔMTB-VI WT-VII
3.
7.
11.
ΔMTB-VI
WT-VII ΔMTA-VI cells + ΔMTB-VI cells
4.
8.
D
Starvation
Pre-incubated
WT
WT-VI WT-VII
ΔMTA-VI WT-VII
1.
4.
7.
20 µm
92% with signal
7% with signal
ΔMTA-VI
WT-VII ΔMTA-VI
ΔMTB-VI WT-VII
2.
5.
8.
87% with signal
0% with signal
ΔMTB-VI
WT-VII ΔMTB-VI
WT-VII ΔMTA-VI cells + ΔMTB-VI cells
3.
6.
9.
0% with signal
89% with signal

Figure 3

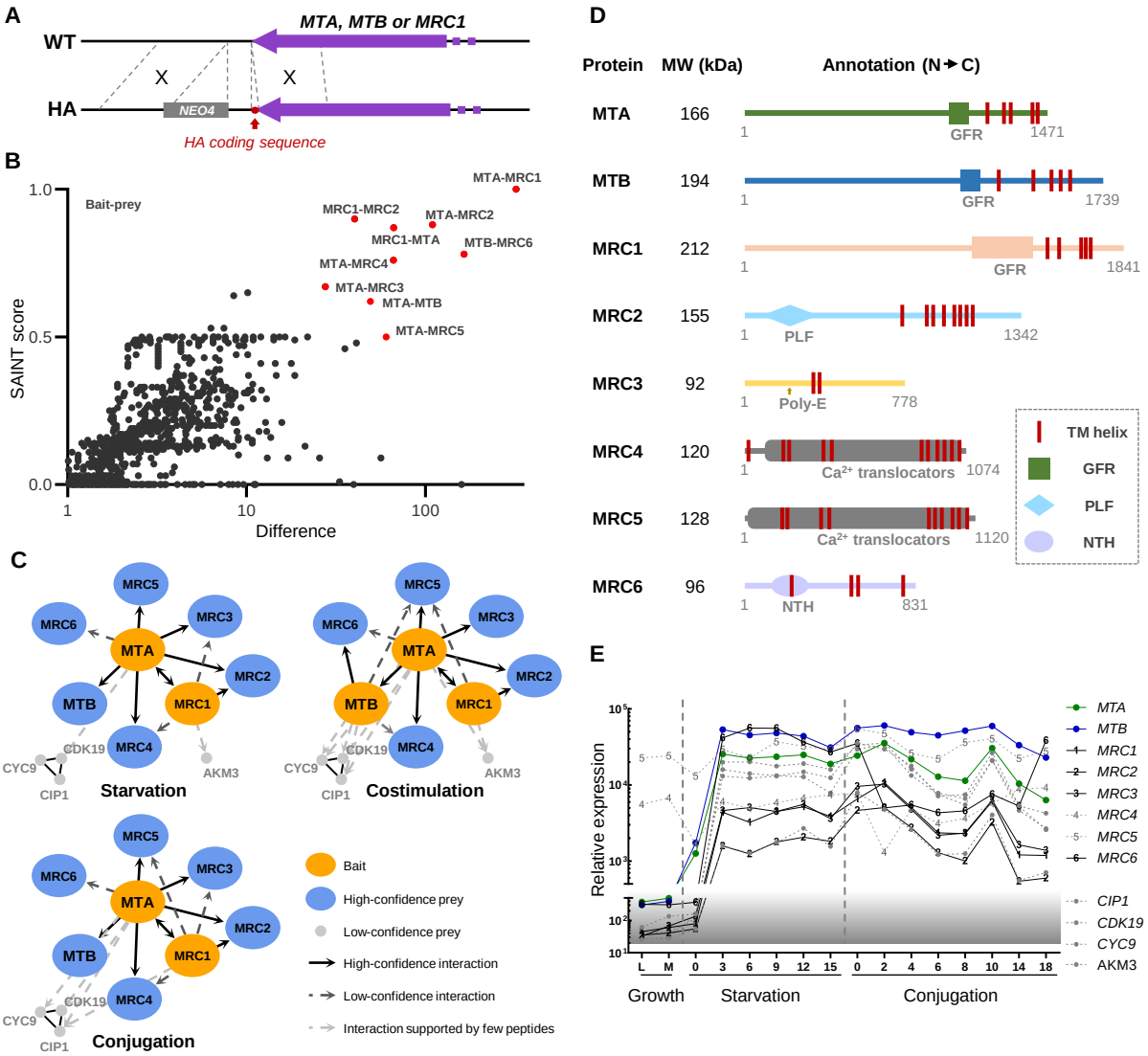
A
WT
MTA, MTB or MRC1
X
X
HA
NEO4
HA coding sequence
B
Bait-prey
SAINT score
Difference
1.0
0.5
0.0
1
10
100
MTA-MRC1
MRC1-MRC2
MTA-MRC2
MRC1-MTA
MTB-MRC6
MTA-MRC4
MTA-MRC3
MTA-MTB
MTA-MRC5
C
MRC5
MRC6
MRC3
MTA
MRC2
MTB
MRC1
CDK19
MRC4
CYC9
CIP1
AKM3
Starvation
Costimulation
Conjugation
Bait
High-confidence prey
Low-confidence prey
High-confidence interaction
Low-confidence interaction
Interaction supported by few peptides
D
Protein
MW (kDa)
Annotation (N→C)
MTA 166 1 GFR 1471
MTB 194 1 GFR 1739
MRC1 212 1 GFR 1841
MRC2 155 1 PLF 1342
MRC3 92 1 Poly-E 778
MRC4 120 1 Ca2+ translocators 1074
MRC5 128 1 Ca2+ translocators 1120
MRC6 96 1 NTH 831
TM helix
GFR
PLF
NTH
E
Relative expression
MTA
MTB
MRC1
MRC2
MRC3
MRC4
MRC5
MRC6
CIP1
CDK19
CYC9
AKM3
L M 0 3 6 9 12 15 0 2 4 6 8 10 14 18
Growth
Starvation
Conjugation

Figure 4

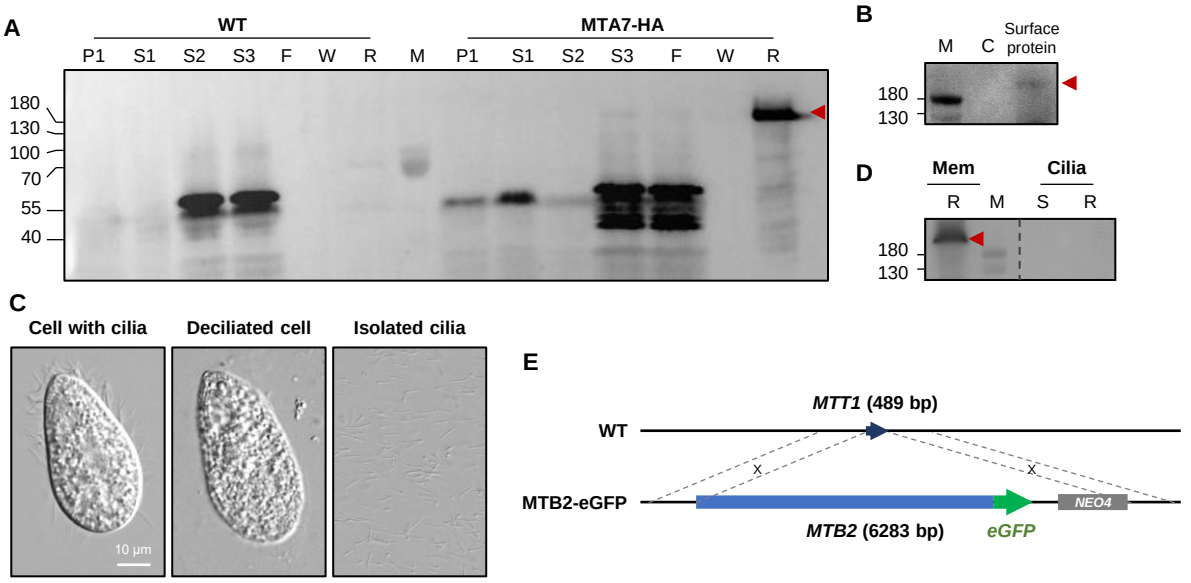
A
WT
MTA7-HA
P1 S1 S2 S3 F W R M P1 S1 S2 S3 F W R
180
130
100
70
55
40
B
M C Surface protein
180
130
D
Mem
Cilia
R M S R
180
130
C
Cell with cilia
Deciliated cell
Isolated cilia
10 µm
E
MTT1 (489 bp)
WT
MTB2-eGFP
NEO4
MTB2 (6283 bp)
eGFP

F

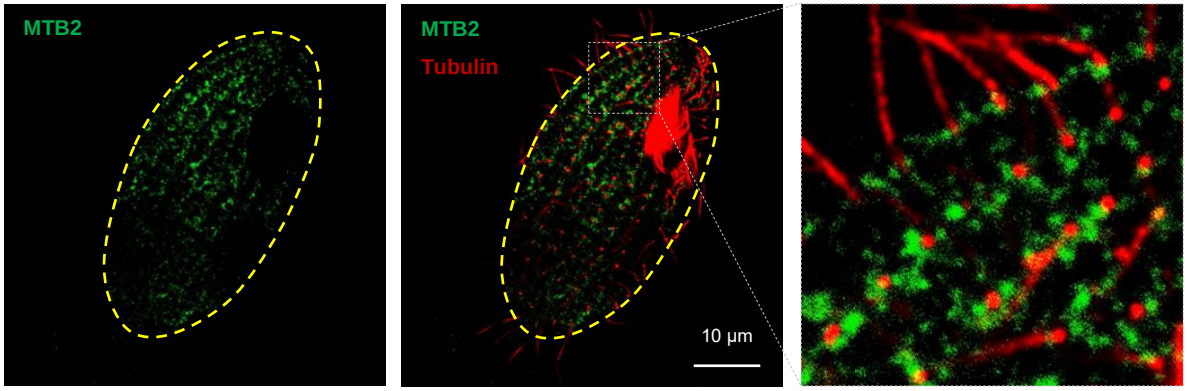
MTB2
MTB2
Tubulin
10 µm

G

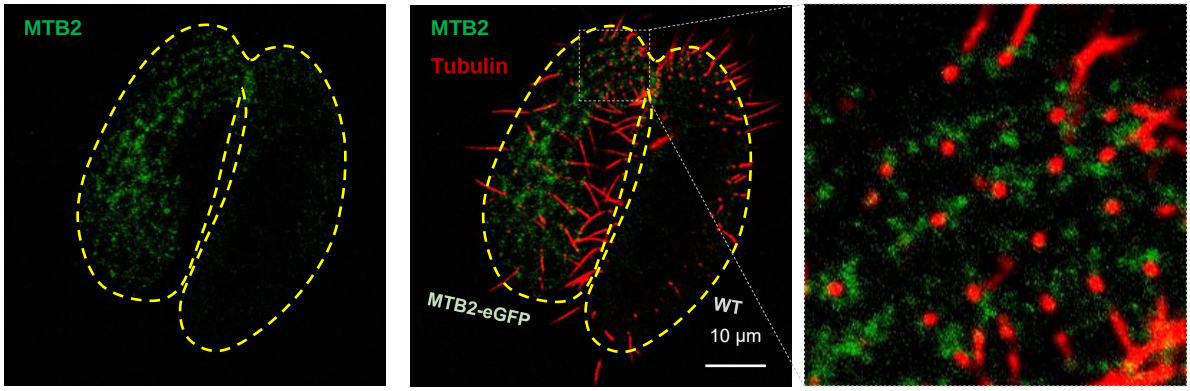
MTB2
MTB2
Tubulin
MTB2-eGFP
WT
10 µm

Figure 5

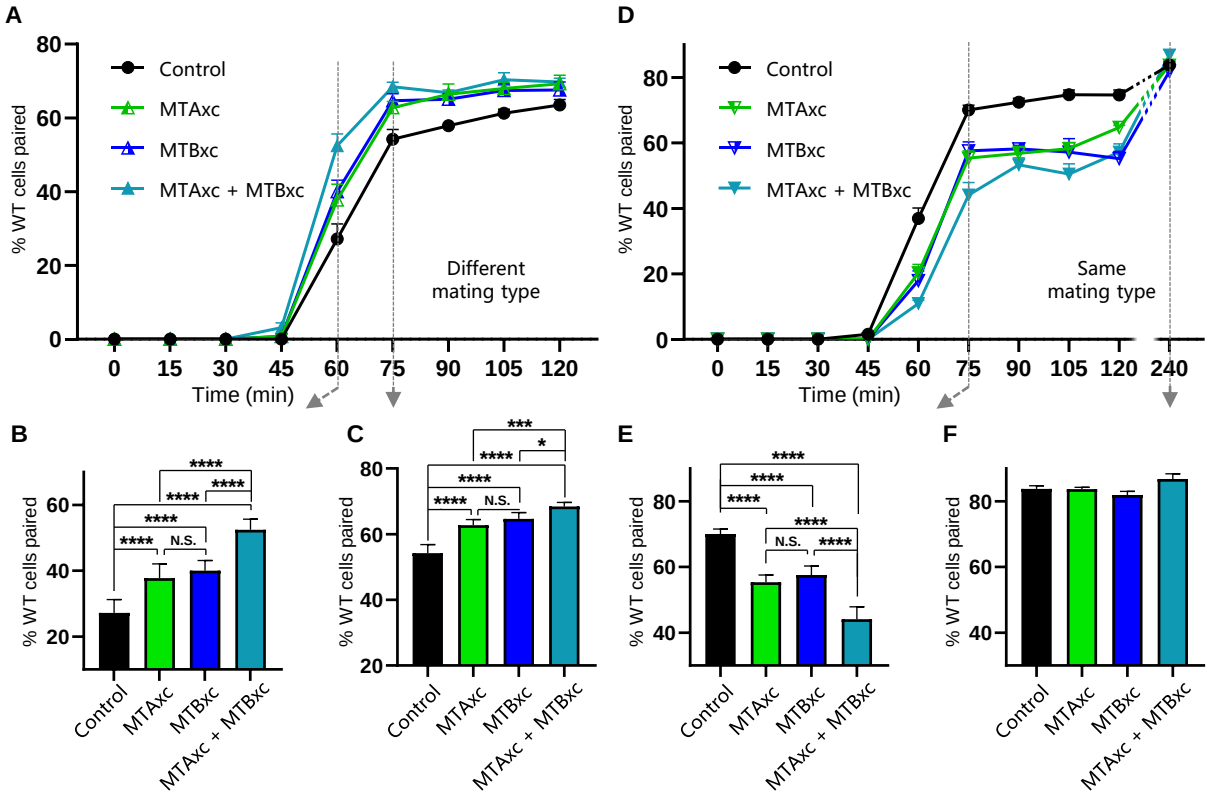
A
% WT cells paired
Control
MTAxc
MTBxc
MTAxc + MTBxc
Different mating type
Time (min)
D
Same mating type
B
C
E
F
N.S.
Control
MTAxc
MTBxc
MTAxc + MTBxc

Figure 6

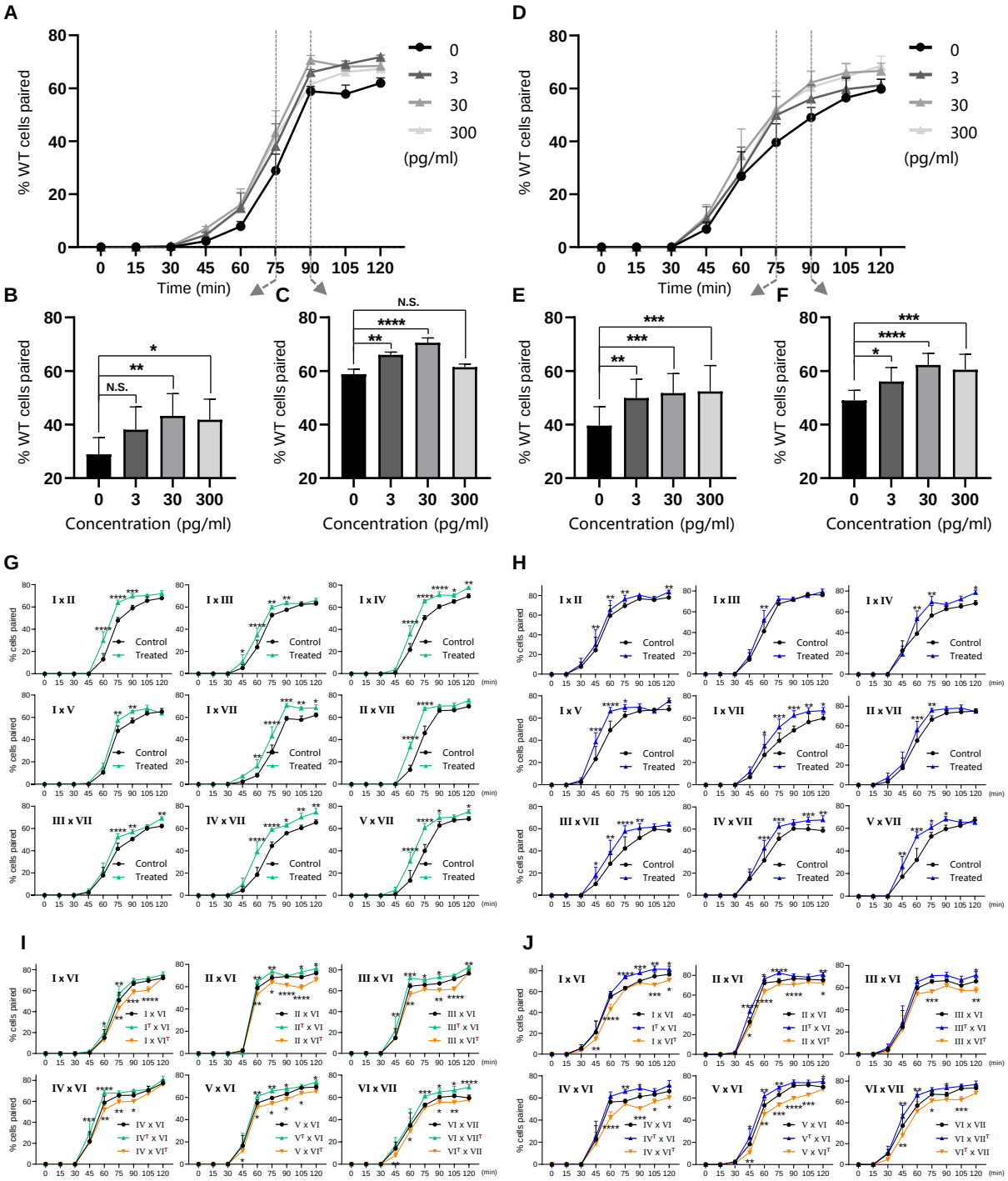
A
% WT cells paired
Time (min)
0
3
30
300
(pg/ml)
D
B
C
E
F
N.S.
Concentration (pg/ml)
G
H
I
J
I x II
I x III
I x IV
I x V
I x VII
II x VII
III x VII
IV x VII
V x VII
I x VI
II x VI
III x VI
IV x VI
V x VI
VI x VII
% cells paired
Control
Treated
(min)

Figure 1 – figure supplement 1

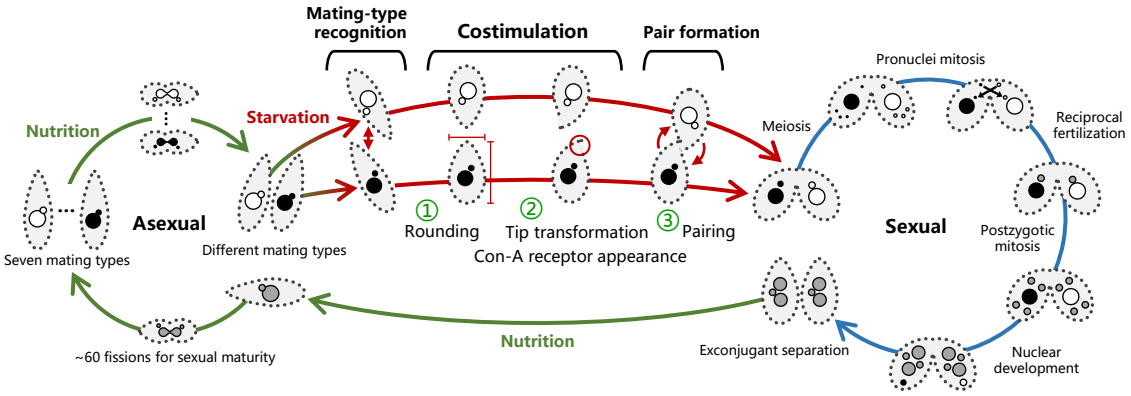

Figure 2 – figure supplement 1

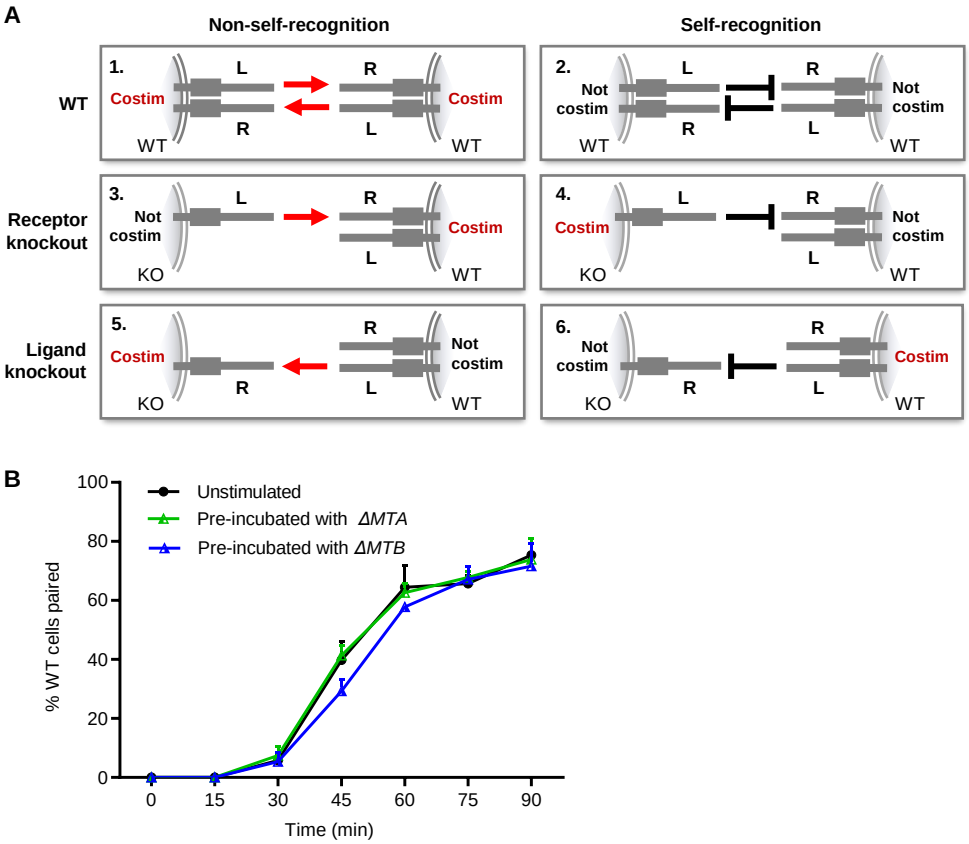

Figure 4 – figure supplement 1

A

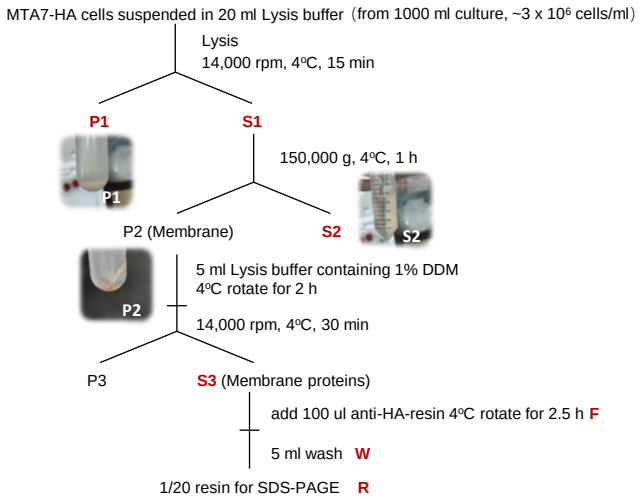

B

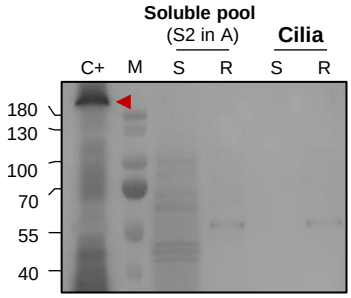

Figure 4 – figure supplement 2

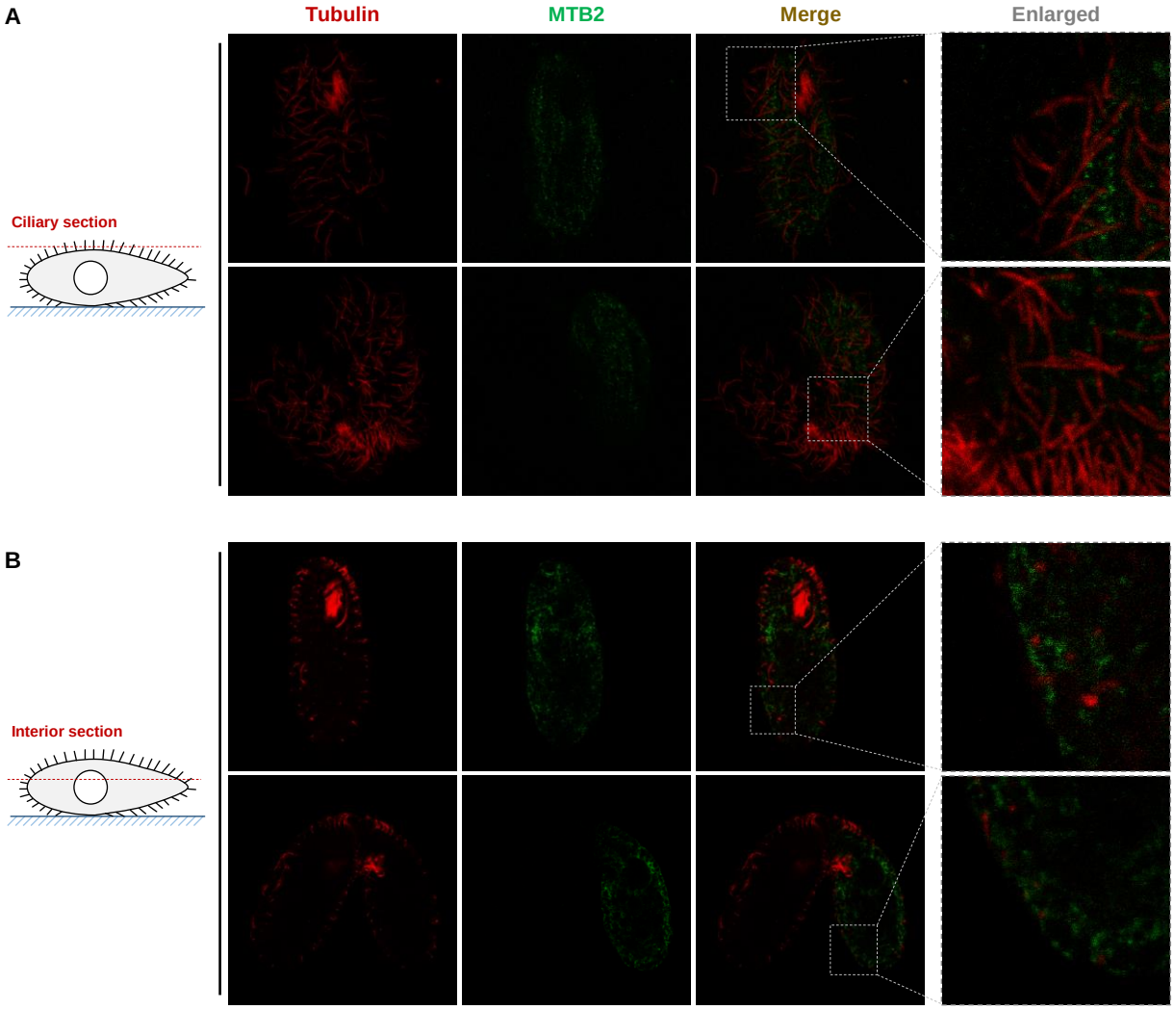

Figure 5 – figure supplement 1

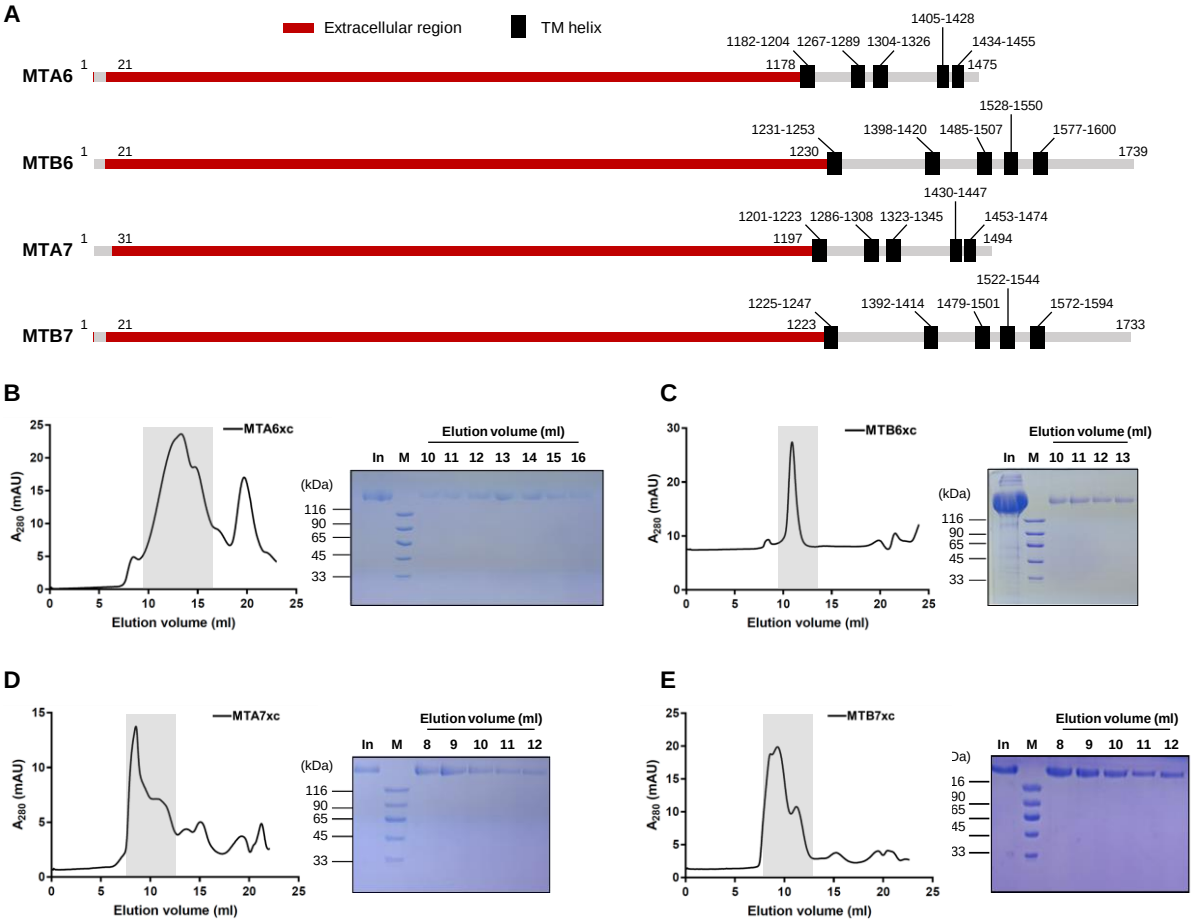
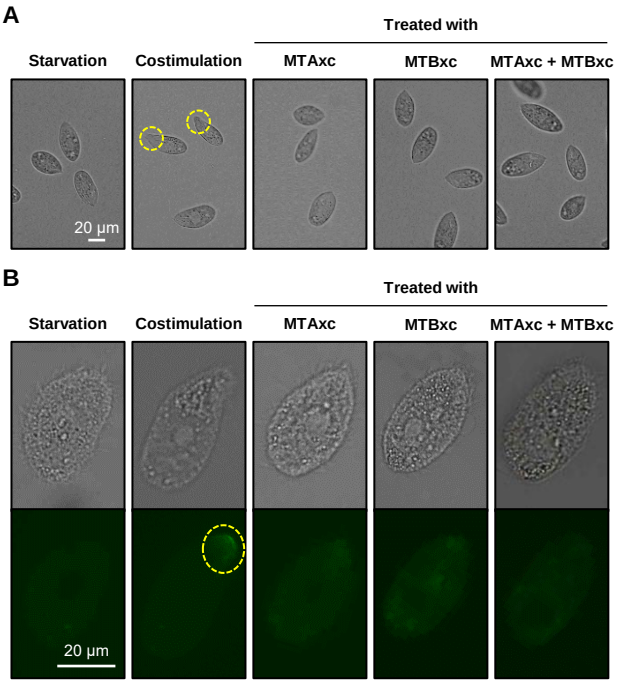
Figure 5 – figure supplement 2